Chemical functionalization of graphene with defects

D. W. Boukhvalov and M. I. Katsnelson

Institute for Molecules and Materials, Radboud University Nijmegen, Heyendaalseweg 135, 6525 AJ Nijmegen, The Netherlands

Abstract

Defects change essentially not only electronic but also chemical properties of graphene being centers of its chemical activity. Their functionalization is a way to modify electronic and crystal structure of graphene which may be important for graphene-based nanoelectronics. Using hydrogen as an example, we have simulated a chemistry of imperfect graphene for a broad class of defects (Stone-Wales defects, bivacancy, nitrogen substitution impurity, and zigzag edges) by density functional calculations. We have studied also an effect of finite width of graphene nanoribbons on their chemical properties. It is shown that magnetism at graphene edges is fragile with respect to oxidation and, therefore, a chemical protection of the graphene edges may be required for application of graphene in spintronics. At the same time, hydrogenation of the Stone-Wales defects may be a perspective way to create magnetic carbon.

Graphene [1, 2, 3] is a novel and very perspective material for nanoelectronics [1, 4]. Effect of various imperfections of the crystal lattice, such as Stone-Wales defects (SW) [5], vacancies [6], substitution atoms [7, 8], etc., on physical properties of graphene was studied theoretically [10, 11, 12, 13]. Recently, first experimental observations of defects in graphene have been reported [14, 15, 16]. Earlier, the defects in carbon nanotubes have been intensively investigated [17, 18, 19, 20, 21]. It is known that defects can influence essentially on chemistry of graphene, and there are several theoretical considerations of chemical functionalization of imperfect graphene [12, 22, 23]; also, the defects were experimentally used as attractors for impurities [15].

It is still unclear, however, what are typical defects in real graphene samples and what is their concentration. Further studies would be important both scientifically and technologically, to find a way to produce defect-free graphene or graphene with desired defects to modify electronic properties, like in conventional semiconductors. The chemical functionalization is probably the most suitable way to detect imperfections in graphene crystal lattice. However, only chemisorption of individual atoms or their pairs were considered before, whereas it was demonstrated that, say, for the case of hydrogenation of ideal graphene a complete coverage turned out to be the energetically most favorable so, the most probably, impurities would tend to form the whole clusters on the top of imperfect graphene [24, 25]. Therefore a systematic study of chemisorption on defects in graphene for a broad range of coverage is desirable; this is the subject of the present work.

Edges of graphene sheets which are broadly discussed now, due to their potential relevance for field-effect transistors and spintronic devices [26, 27, 28, 29, 30, 31, 32] can be also considered as defects. Their functionalization and its effect on the electronic structure were discussed in a series of theoretical works [31, 33, 34, 35, 36, 37, 38, 39, 40, 41], chemical activity of the graphene edges being discussed [42], but only the chemical functionalization of the edges themselves were considered rather than of the whole graphene sheet *with* the edges. Actually, the edges change chemical activity of graphene in an extended region, as will be demonstrated here. This is important to study stability of magnetism at the edges and to evaluate a width of a "near-edge layer" where properties of graphene are essentially different from those in the bulk.

We will use hydrogenation as an example of the chemical functionalization of defects in graphene. For the case of ideal graphene general factors determining the chemisorption were first studied for the case of hydrogen [24] and appeared to be applicable also in other situations, such as graphene oxide [25]. One can expect therefore that, at least, some of peculiarities which are found here can be of a more general relevance.

We used the pseudopotential density functional SIESTA package for electronic structure calculations [43, 44] with the generalized gradient approximation for the density functional [45], with energy mesh cutoff 400 Ry, and k-point 8×8×2 mesh in Monkhorst-Park scheme [46] for modeling of defects, and 2×12×2 for modeling of nanoribbons. During the optimization, the electronic ground state was found self-consistently by using norm-conserving pseudopotentials for cores and a double-ζ plus polarization basis of localized orbitals for carbon and oxygen, and double-ζ one for hydrogen. Optimization of the bond lengths and total energies was performed with an accuracy 0.04 eV /Å and 1 meV, respectively. This method is frequently used for computations of electronic structure of graphene [9, 28, 29, 24, 25]. When drawing the pictures of density of states, a smearing by 0.2 eV was used.

Chemisorption energies were calculated by standard formulas used, e.g., earlier for the cases of chemisorption of hydrogen [24] oxygen and hydroxyl groups [25] on graphene and solution of carbon in γ-iron [47]. Thus, energy of the chemisorption of single hydrogen atom at graphene with Stone-Wales defect (Fig. 1a) was calculated as

E_{form}=E_{SW+H}-E_{SW}-E_{H_2}/2 where E_{SW+H} was the total energy of the supercell with chemisorbed hydrogen found by self-consistent calculations after optimization of geometric structure, E_{SW} was the total energy of the graphene supercell with the Stone-Wales defect found in a similar way, and E_{H_2} is the energy of hydrogen molecule. The latter choice describes the most adequately a process of spontaneous hydrogen dissociation and, thus, stability of graphene with respect to the hydrogenation. That is why this definition is broadly used when discussing hydrogen storage [48, 49]. In principle, a definition of the hydrogenation energy depends on what specific compound is used for the hydrogenation. This may shift the chemisorption energy values of hydrogen in Figs. 2, 4, 9, and 10. For example, for the hydrogenation by hydrogen plasma all formation energies presented below will be lower by 104.206 kcal/mol, or 2.255 eV per atom, which is the experimental bond dissociation energy for H_2.

We used graphene supercell containing 50 carbon atoms, similar to that used in our previous work [24]. It was demonstrated there that the chemisorption energy for two hydrogen atoms is close to that for two independent single atoms if the distance between the atoms is larger than 1 nm (approximately, four graphene lattice constants). Similar results have been obtained for the case of hydroxy groups [25]. This means that a supercell provided the distance between defects larger than 1 nm is sufficient to model the chemisorption on individual defects.

Optimized geometric structures of graphene supercells with various kinds of defects are presented in Fig. 1. To simulate graphene nanoribbons we used the stripes with 22, 44, and 66 carbon atoms per cell, with the width 2.20, 4.54, and 6.88 nm, respectively.

We start with the calculations of activation energy, that is, the chemisorption of a single hydrogen atom. For pure graphene this energy is 1.5 eV [24] and for all kind of defects under consideration it turns out to be lower, namely, 0.30 eV for SW, 0.93 eV for bivacancy, and 0.36 eV for substitution impurity of nitrogen (in the latter case we mean the energy of chemisorption on a carbon neighbor of the nitrogen impurity).

We have calculated also the chemisorption energy for different nonequivalent atoms of the lattice containing the SW defect (Fig. 2a). One can see that the chemisorption energy at the SW defect is minimal. At the same time, in a whole area surrounding the defect the chemisorption energy is lower than in perfect graphene [24]. For distant enough atoms the energy is very close to the values found in Ref. [24] which confirms that the supercell with 50 atoms is sufficient to describe the chemisorption on the single defect.

The computational results mean that defects in graphene are centers of chemical activity. As a next step, we investigate an interaction of a pair of hydrogen atoms with defects (Fig. 3a). Again, the defects decrease the chemisorption energy of the pair in comparison with the case of ideal graphene. We have calculated also the pair formation energy for the case when the first hydrogen atom is chemisorbed on the SW defect and the second one - on one of the surrounding carbon atoms (Fig. 2b). The chemisorption energies are presented there for the case of one-side chemisorption; for the first and second neighbors of the SW defect the one-side chemisorption is energetically more favorable [12, 22, 23] whereas for farther atoms the difference with the two-side chemisorption energies becomes negligible [24]. Similar to the case of single hydrogen atom discussed above a region is formed around the defect with a diameter of order of 1 nm where the chemisorption energies are lower than in the bulk.

These results may be essential for the problem of magnetism in graphene. Chemisorption of a single hydrogen atom on graphene results in appearance of magnetic moments [12, 50, 51] whereas close hydrogen pairs on graphene turn out to be nonmagnetic, the pairs being more energetically favorable than independent atoms [24, 52, 53]. At the same time, there is an energy barrier which two distant hydrogen atoms on graphene should overcome to form the pair [54]. If one of these atoms are bonded with the SW defect the barrier becomes higher by 0.44 eV which makes the pair formation at room temperature rather difficult. Thus, the hydrogenation of the SW defects may be a perspective way to create magnetic graphene. It can be done, for example, using reactions with superacids, similar to the case of fullerenes [55].

For SW and bivacancies the chemisorption energy of single hydrogen atom is negative which makes these defects centers of *stable* chemisorption of hydrogen. At further increase of the number of hydrogen atoms the chemisorption energy decreases reaching a minimum for the most stable configuration (for the case of SW it is shown in Fig. 3b), then increases up to a local maximum (the corresponding structure is shown in Fig. 3c) and then decreases again, with the global minimum for complete coverage. Contrary, in the case of ideal graphene the chemisorption energy decreases monotonously with the hydrogen concentration and clusters of chemisorbed hydrogen are not stable [56]. Interestingly, for the case of complete coverage the binding energy is smaller for the hydrogen on graphene with defects than on the perfect one. This means that completely hydrogenated graphene (graphane [24, 57]) is less stable with defects than without them.

Our results show that, whereas at the hydrogenation of pure graphene there is single potential barrier to overcome, that is, the adsorption of the first atom, for imperfect graphene several barriers can exist (see Fig. 4). The first one, again, corresponds to the activation energy and the other ones - to the transition

from hydrogenation of the region around defect with the minimal chemisorption energy (see Fig. 2) to the hydrogenation of the whole graphene sheet. Studying experimentally kinetics of this process one can extract an information about presence of defects in graphene and their type. At the same time, graphene with defects can be a good model of activated carbon [58, 59]. The fact that the adsorption and desorption energies are smaller than 0.5 eV per hydrogen atom makes graphene with defects a perspective catalyst.

Let us consider now the hydrogenation of graphene edges. We focus on the zigzag edges which are especially interesting due to their possible half-metallic ferromagnetic state [28, 29, 30]. For the nanoribbons of width 2.20, 4.54, and 6.88 nm, the chemisorption energies for a single hydrogen atom (Fig. 5b) are found to be -2.39, -2.76, and -2.82 eV, respectively. High chemical activity of the edges, in comparison with the bulk graphene [24] is explained by a presence of unpaired electrons due to broken bonds (Fig. 5a). Only one unpaired electron is involved in the bond with the single hydrogen atom whereas the second one can participates in the second bond (Fig. 5c). The chemisorption of the second hydrogen atom leads to strong local distortions of graphene, due to a change of hybridization from sp^2 (favorable for a planar geometry) to sp^3 (favorable for three-dimensional structure like in diamond). These distortions require some energy which is higher than the energy gain due to pairing of all electrons and, as a result, an energy barrier about 1.5 eV is formed for all nanoribbons under investigation. The cohesive energy of pure graphene is rather strongly dependent on the ribbon width (Fig. 6). This result in a strong dependence of the chemisorption energy on the ribbon width as well. The energy of chemisorption of two hydrogen atoms at the edges is negative, in contrast with the case of perfect bulk graphene [24] which makes the edges another natural centers of chemical activity. Similarly, zigzag edges can adsorb two fluorines [61], or two hydroxyl groups, or a pair of hydroxyl group and hydrogen, the latter case being related to the decomposition of a water molecule (Fig. 7). The formation energy per H_2O molecule corresponding to this process is -2.42 eV (241 kJ/mol) for the ribbon width 2.20 nm which makes the decomposition of the water more favorable than the chemisorption of single hydrogen atom.

In a case of chemisorption of oxygen atoms, both unpaired electrons are involved but the hybridization remains sp^2 and local geometry therefore remains flat (Fig. 5d). The chemisorption energy for the oxygen atom is much lower than for hydrogen or hydroxyl; for the ribbon width 2.2 nm it turns out to be -4 eV. Recently, peaks corresponding to C=O chemical bonds have been found in the core-level spectra of carbon in graphene nanoribbons [60]. They were related to edge groups, based on ratio of intensities of these peaks and of the main peaks corresponding to sp^2 hybridization.

Since all unpaired electrons are bonded at the complete oxygenation of the edge, the magnetism disappears and electronic structure becomes purely metallic (see Fig. 8), instead of half-metallic ferromagnetic for undoped zigzag edges [28]. Note that the decomposition of the water molecule described above will also suppress the magnetism of the zigzag edges, as was observed at fluorination of the graphene edges [61].

Now we consider further hydrogenation of graphene, from the edges to bulk. The computational results presented in Fig. 9 show that the chemisorption of hydrogen is the most energetically favorable near the edges and less favorable in the middle of the nanoribbon where the formation energy is close to that for the bulk (1.44 eV [24]). The chemisorption energy is very sensitive to the distortions created by adsorbed hydrogen atoms. It was shown earlier for the bulk graphene [24] that the difference in chemisorption energies for different configurations of a pair of hydrogen atoms can be as large as 0.45 eV. In graphene nanoribbons these effects seem to be even stronger. In particular, geometric frustrations due to the atomic distortions lead to a zigzag dependence of the chemisorption energy on atomic position (Fig. 9). At the chemisorption of single hydrogen atom interactions between the hydrogen-induced distortions and those due to edge itself is important. This effect decays when moving from the edge at distances of order of 1 nm. As well as in the case of SW defect, the pair formation can be more difficult for the nanoribbon than for bulk graphene, due to larger barrier energy. This may be essential, again, for the problem of hydrogen-induced magnetism in graphene.

The results are shown in Fig. 10. One can see that, irrespective to the ribbon width, at first the formation energy grows by steps which corresponds to a preferable hydrogenation of graphene by pairs of atoms [24]. This growth continues at the depth of 8 carbon atoms (0.85 nm, which is slightly larger than for the single atom due to two-side hydrogenation) and then the energy increases approximately linearly with the coverage, as in the case of infinite graphene sheet [24]. This means that the hydrogenation of graphene proceeds in three steps, namely, the hydrogenation of the edge, then, of the near-edge layer with a width of order 1 nm, and, at last, of the bulk. The chemical functionalization of the near-edge layer effects essentially on the electronic structure of graphene nanoribbons (see Fig. 8). It is worth to note that for the ribbons under consideration the hydrogenation energy is negative which makes them chemically active in their whole area. This can influence the electronic structure as was mentioned earlier [26].

To conclude, let us summarize the main results. Defects in graphene crystal lattice, as well as the edges of graphene, change drastically a scenario of its chemical functionalization. For the ideal graphene, only sin-

gle energy barrier related with the chemisorption of the first atom is relevant and complete functionalization corresponds to the global energy minimum. At the same time, for "realistic" graphene with imperfections and edges local energy minima are formed corresponding to local functionalization of a region with radius of order half of nanometer and further functionalization is stopped by presence of another energy barrier. The local energy minima make migration of chemisorbed atoms and groups more difficult. In the cases of hydrogen and other atoms and groups with single unpaired electron, this can stabilize a magnetic state preventing formation of nonmagnetic pairs. We have found that magnetic state of edges in graphene nanoribbons may be unstable with respect to oxidation and water dissociation at the edges. Therefore, keeping in mind potential applications of this magnetism in spintronics special methods of chemical protection of the edges should be developed.

Acknowledgment The work is financially supported by Stichting voor Fundamenteel Onderzoek der Materie (FOM), the Netherlands.

References

[1] Geim, A. K.; Novoselov, K. S. *Nature Mater.* **2007**, *6*, 183.

[2] Katsnelson, M. I. *Mater. Today* **2007**, *10*, 20.

[3] Castro Neto, A. H.; Guinea, F.; Peres, N. M. R.; Novoselov, K. S.; Geim, A. K. *Rev. Mod. Phys.*, in print; arXiv:0709.1163.

[4] Ponomarenko, L. A.; Schedin, F.; Katsnelson, M. I.; Yang, R.; Hill, E. W.; Novoselov, K. S.; Geim, A. K. *Science*, **2008**, *320*, 356.

[5] Stone, A. J.; Wales, D. J. *Chem. Phys. Lett.* **1986**, *128*, 501.

[6] Carlson, J.M.; Scheffler, M. *Phys. Rev. Lett.*, **2006**, *96*, 046806.

[7] Zhu, Z. H.; Hatori, H.; Wang, S. B.; Lu, G. Q. *J. Phys. Chem. B* **2005**, *109*, 16744.

[8] Miwa, R. H.; Martins, T. B. Fazzio, A. *Nanotechnology* **2008**, *19*, 155708.

[9] Li, L.; Reich, S.; Robertson, J. *Phys. Rev. B* **2005**, *72*, 184109.

[10] Cortijo, A.; Vozmediano, M. A. H. *Europhys. Lett.* **2007**, *77*, 47002.

[11] Carpio, A.; Bonilla, L. L.; de Juan, F.; Vozmediano, M. A. H. *New J. Phys.* **2008**, *10*, 053021.

[12] Duplock, E.J.; Scheffler, M.; Lindan, P.J.D. *Phys. Rev. Lett.*, **2004**, *92*, 225502.

[13] Lherbier, A.; Blase, X.; Niquet, Y.-M.; Triozon, N.; Roche, S. *Phys. Rev. Lett.* **2008**, *101*, 036808.

[14] Meyer, J.; Kiselowski, C.; Rossell, M. D.; Crommine, M. F.; Zettl, A. *Nano Lett.* **2008**, , in press.

[15] Wang, X.; Tabakman, S. M.; Dai, H. *J. Am. Chem. Soc* **2008**, *130*, 8152.

[16] Coleman, V. A.; Knut, R.; Karis, O.; Grennberg, H.; Jansson, U.; Quinlan, R.; Holloway, B. C.; Sanyal, B.; Eriksson, O. *J. Phys. D: Appl. Phys.* **2008**, *41*, 062001.

[17] Zhou, O.; Fleming, R. M.; Murphy, D. W.; Chen, C. H.; Haddon, R. C.; Ramirez, A. P.; Glarun, S. H. *Science* **1994**, *263*, 1744.

[18] Carrero-Sanchez, J. C.; Elias, A. L.; Mancilla, R.; Arrellin, G.; Terrones, H.; Laclette, J. P.; Terrones, M. *Nano Lett.* **2006**, *6*, 1609.

[19] Terrones, M.; Redlich, P.; Grobert, N.; Trasobares, S.; Hsu, W.-K.; Terrones, H.; Zhu, Y.-Q.; Hare, J. P.; Reeves, C. L.; Cheetham, A. K.; Rühle, M.; Kroto, H. W.; Walton, D. R. M. *Adv. Mater.* **1999**, *11*, 655.

[20] Miyamoto, Y.; Rubio, A.; Berber, S.; Yoon, M.; Tománek, D. *Phys. Rev. B* **2004**, *69*, 121413(R).

[21] Krasheninnikov, A. V.; Banhart, F. *Nat. Mater.* **2007**, *6*, 723.

[22] Letardi, S.; Celino, M.; Cleri, F.; Rosato, V. *Surf. Sci.* **2002**, *496*, 32.

[23] Yang, F. O.; Huang, B.; Li, Z.; Xu, H. *J. Phys. Chem. C*, **2008**, *112*, 1200.

[24] Boukhvalov, D. W.; Katsnelson, M. I.; Lichtenstein, A. I. *Phys. Rev. B* **2008**, *77*, 035427.

[25] Boukhvalov, D. W.; Katsnelson, M. I.; *J. Am. Chem. Soc.* **2008**, *130*, 10697.

[26] Wang, X.; Ouyang, Y.; Li, X.; Wang, H.; Guo, J.; Dai, H. *Phys. Rev. Lett* **2008**, *100*, 206803.

[27] Li, X.; Wang, X.; Zhang, L.; Lee, S.; Dai, H. *Science* **2008**, *319*, 1229.

[28] Son, Y.-W.; Cohen, M. L.; Loui, S. G. *Nature (London)* **2006**, *444*, 347.

[29] Wang, W. L.; Meng, S.; Kaxiras, E. *Nano Lett.* **2008**, *8*, 241.

[30] Yazyev, O. V.; Katsnelson, M. I. *Phys. Rev. Lett.* **2008**, *100*, 047209.

[31] Yang, L.; Park, C. H.; Son, Y. W.; Loui, S. G. *Phys. Rev. Lett.* **2007**, *99*, 186801

[32] Kan, E.; Li, Z.; Yang, J.; Hou, J. G. *Appl. Phys. Lett.* **2008**, *91*, 243116.

[33] Servantes-Sodi, F.; Csány, G.; Pisanec, S.; Ferarri, A. C. *Phys. Rev. B***2008**, *77*, 165427.

[34] Hod, O.; Barone, V.; Perlata, J. E.; Scuseria, G. E. *Nano Lett.* **2007**, *7*, 2295.

[35] Hod, O.; Barone, V.; Scuseria, G. E. *Phys Rev B* **2008**, *77*, 035411.

[36] Hod, O.; Perlata, J. E.; Scuseria, G. E. *Phys. Rev. B* **2007**, *76*, 233401.

[37] Barone, V.; Hod, O.; Scuseria, G. E. *Nano Lett.* **2006**, *6*, 2748.

[38] Huang, B.; Liu, F.; Wu, J.; Gu, B.-L.; Duan, W. *Phys. Rev. B* **2008**, *77*, 153411.

[39] Jiang, D.; Stumper, B. G.; Dai, S. *J. Chem. Phys.* **2007**, *127*, 124703.

[40] Kan, E.; Li, Z.; Yang, J.; Hou, J. G. *J. Am. Chem. Soc.* **2008**, *130*, 4224.

[41] Veiga, R. G. A.; Miwa, R. H.; and Srivastava, G. P. *J. Chem. Phys.* **2008**, *128*, 201101.

[42] Jiang, D.; Stumper, B. G.; Dai, S. *J. Chem. Phys.* **2007**, *126*, 134701.

[43] Artacho, E.; Gale, J.D.; Garsia, A.; Junquera, J.; Martin, R. M.; Orejon, P.; Sanchez-Portal, D.; Soler, J. M. *SIESTA, Version 1.3, 2004*.

[44] Soler, J. M.; Artacho, E.; Gale, J. D.; Garsia, A.; Junquera, J.; Orejon, P.; Sanchez-Portal, D. *J. Phys.: Condens. Matter*, **2002**, *14*, 2745.

[45] Perdew, J. P.; Burke, K.; Ernzerhof, M. *Phys. Rev. Lett.*, **1996**, *77*, 3865.

[46] Monkhorst, H. J.; and Park, J. D. *Phys. Rev. B* **1976**, *13*, 5188.

[47] Boukhvalov, D. W.; Gornostyrev, Yu. N.; Katsnelson, M. I.; Lichtenstein, A. I. *Phys. Rev. Lett.* **99**, *2007*, 247205.

[48] Dillon, A. C.; Jones, K. M. Bekkedahl, T. A. Kiang, C. H.; Bethune, D. S.; Heben, M. J. *Nature (London)* **1997**, *386*, 377.

[49] Dillon, A. C.; Heben, M. J. *Appl. Phys. A* **2001**, *72*, 133.

[50] Lehtinen, P. O.; Foster, A. S.; Ma, Y.; Krasheninnikov, A. V.; Niemien, R. M. *Phys. Rev. Lett.* **2004**, *93*, 187202.

[51] Wessely, O.; Katsnelson, M. I.; Nilsson, A.; Nikitin, A.; Ogasawara, H.; Odelius, M.; Sanyal, B.; Eriksson, O. *Phys. Rev. B* **2007**, *76*, 161402.

[52] Roman, T.; Diño, W. A.; Nakanishi, H.; Kasai, H.; Sugimoto, T.; Tange, K. *Jap. J. Appl. Phys.* **2006**, *45*, 1765.

[53] Roman, T.; Diño, W. A.; Nakanishi, H.; Kasai, H.; Sugimoto, T.; Tange, K. *Carbon* **2007**, *45*, 218.

[54] Jeloaica, L.; Sidis, V. *Chem. Phys. Lett* **1999**, *300*, 157.

[55] Reed, C. A.; Kim, K.-C.; Bolskar, D.; Mueller, L. J. *Science* **2000**, *289*, 101.

[56] Hornekær, L.; Xu, W.; Otero, R.; Lægsgaard, E.; Besenbacher, F.; *Chem. Phys. Lett.* **2007**, *446*, 237.

[57] Sofo, J. O.; Chaudhari, A. S.; Barber, G. D.; *Phys. Rev.B* **2007**, *75*, 153401.

[58] Boehm, H. P. *Carbon* **1994**, *32*, 759.

[59] Gamby, J.; Taberna, P. L.; Simon, P.; Fauvarque, J. F.; Chesneau, M. *J. Power Sourses* **2001**, *101*, 109.

[60] Campos-Delgado, J.; Romo-Herrera, J. M.; Jia, X.; Cullen, D. A.; Muramatsu, H.; Kim, Y. A.; Hayashi, T.; Ren, Z.; Smith, D. J.; Okuno, Y.; Ohba, T.; Kanoh, H.; Kaneko, K.; Endo, M.; Terrones, H.; Dresselhaus, M. S.; Terrones, M. *Nano Lett.* **2008**, *8*, 2773.

[61] Takai, K.; Sato, H.; Enoki, T.; Yoshida, N.; Okino, F.; Touhara, H.; Endo, M. *J. Phys. Soc. Jpn.* **2001**, *71*, 175.

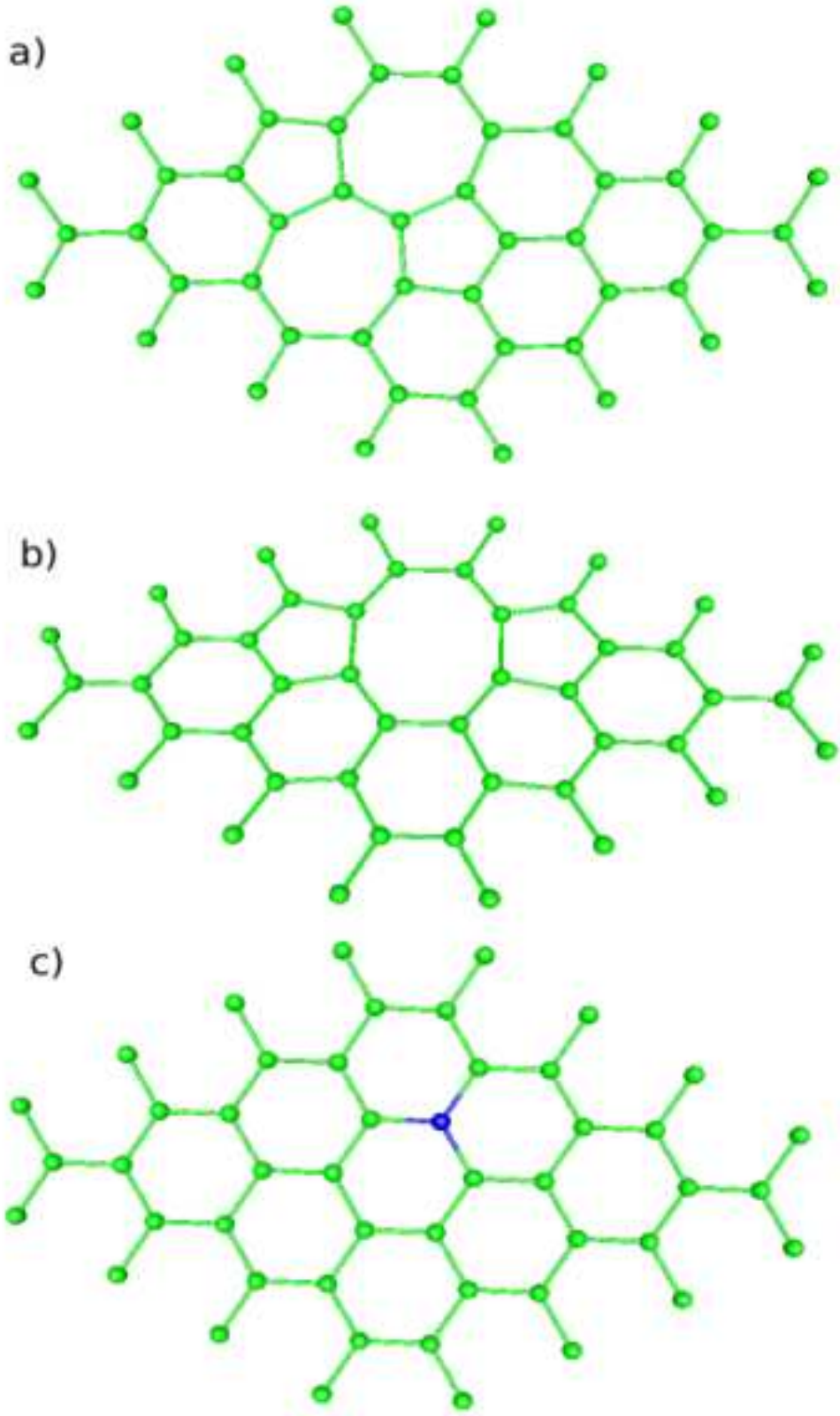

Figure 1: Optimized geometric structures for graphene supercell containing the Stone-Wales defect (a), bivacancy (b), and nitrogen substitution impurity (c).

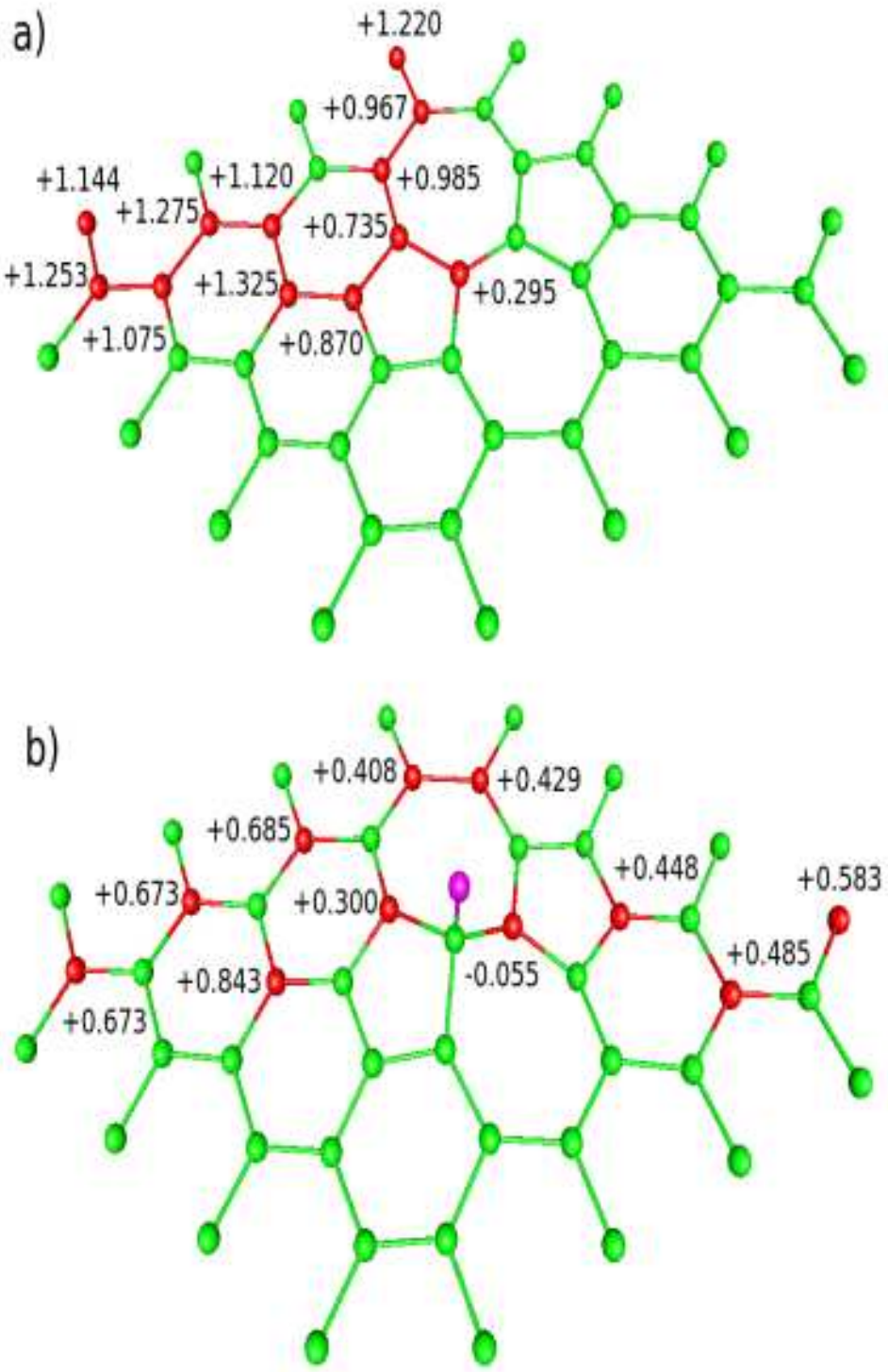

Figure 2: Formation energies (in eV per hydrogen atom) for nonequivalent sites (red circles) of graphene lattice with the SW defect for chemisorption of the first (a) and second (b) hydrogen atoms.

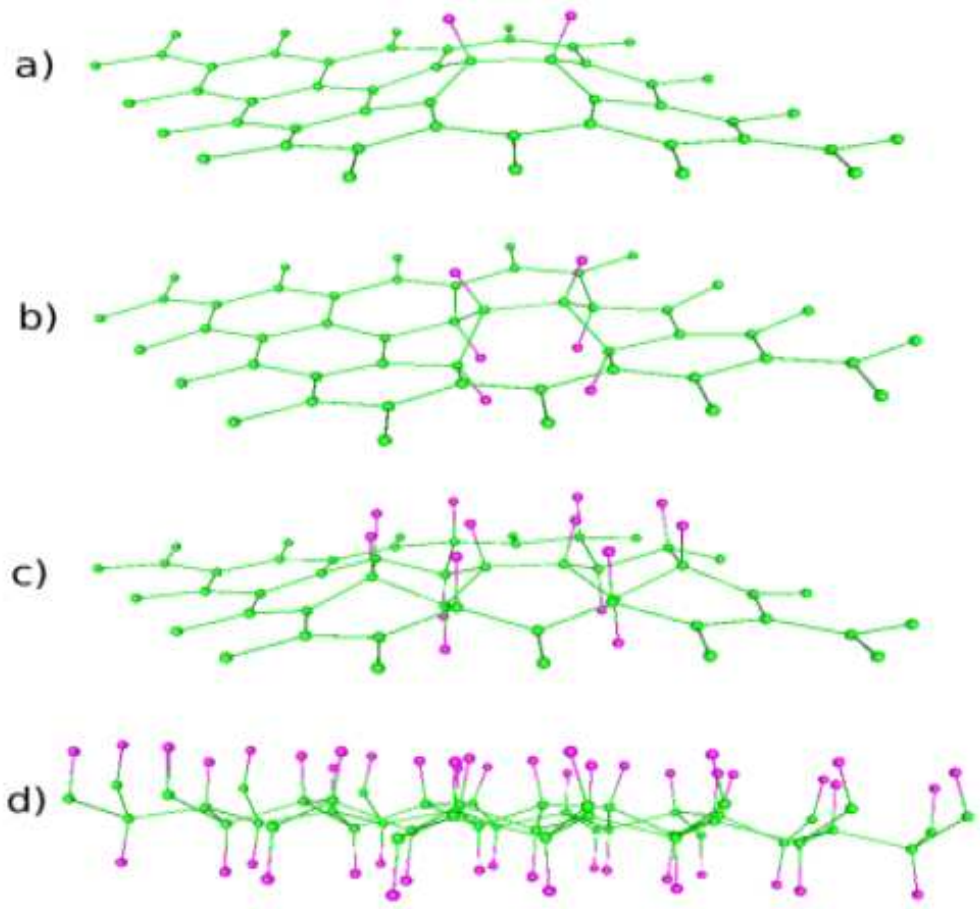

Figure 3: Optimized geometric structures for the Stone-Wales defect functionalized by 2 (a), 6 (b), 14 (c) hydrogen atoms and completely covered by hydrogen (d). Carbon and hydrogen atoms are shown by green and violet circles, respectively.

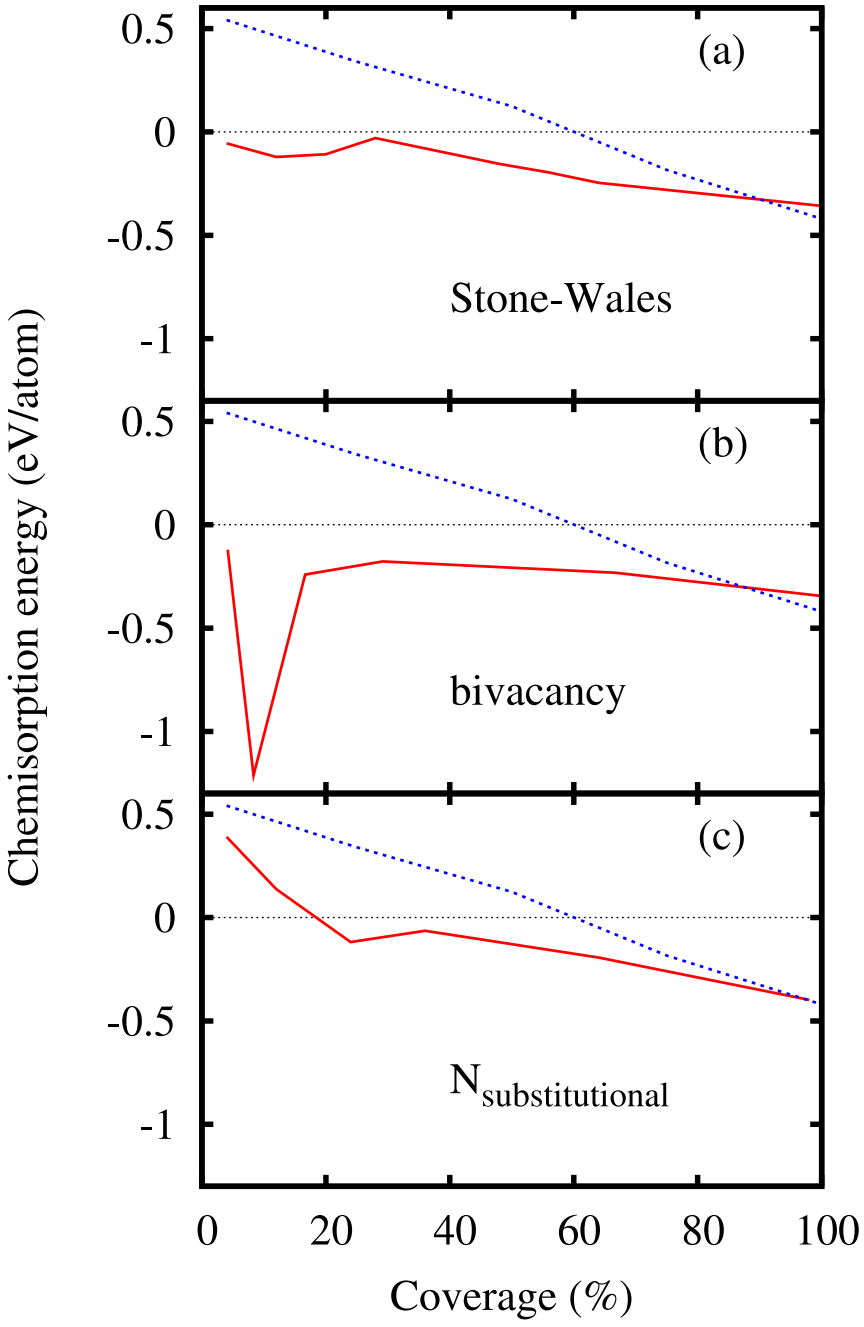

Figure 4: Energy formation as a function of coverage for grapehne sheet containing the Stone-Wales defect (a), bivacancy (b), and nitrogen substitution impurity (c). The blue dashed line represents the results for the ideal infinite graphene sheet.

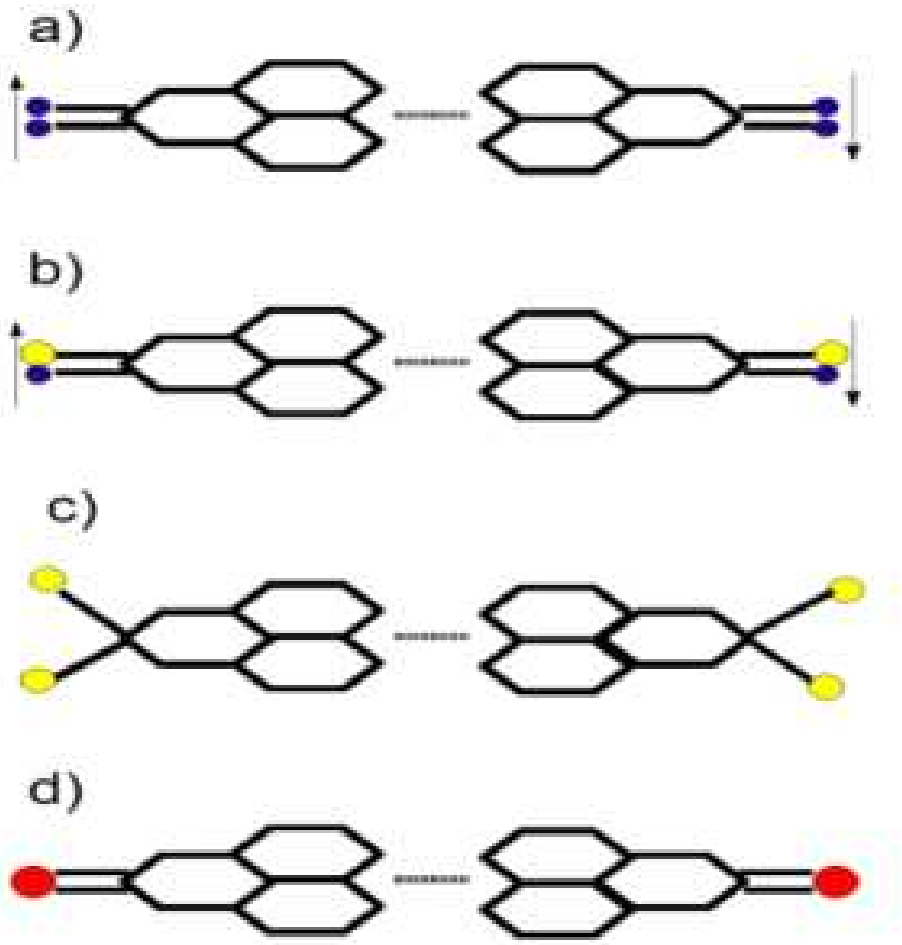

Figure 5: A sketch of functionalization of the zigzag edges of graphene: (a) Initial state of edges, unpaired electrons are shown in blue; (b), (c), and (d) the edge functionalized by a single carbon atom (yellow), by pair of hydrogen atoms, and by oxygen atom (red), respectively.

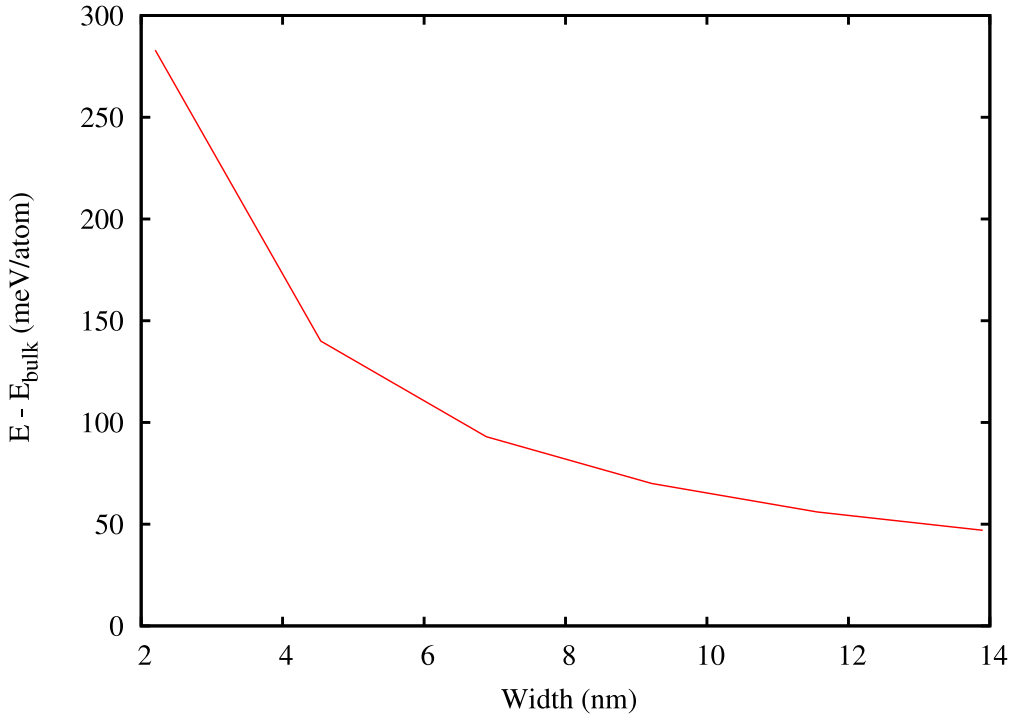

Figure 6: Total energy difference between infinite graphene sheet and graphene nanoribbon as a function of the nanoribbon width.

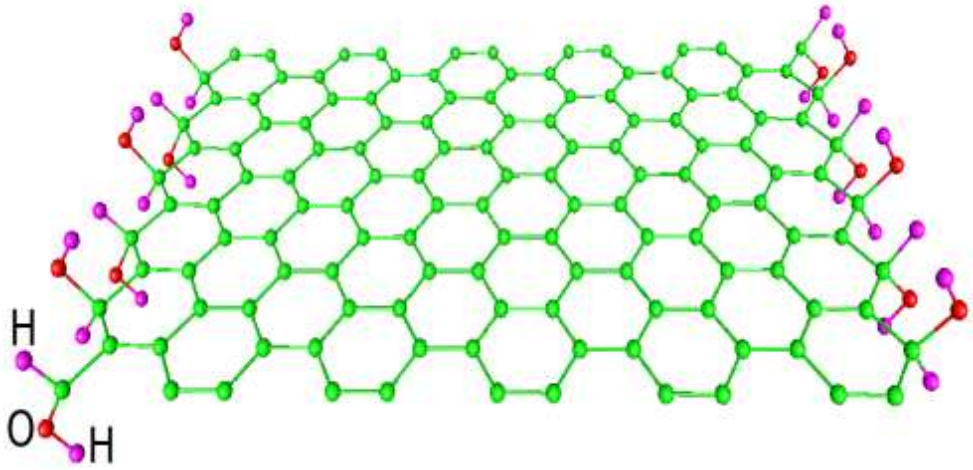

Figure 7: Optimized geometry of the graphene nanoribbon of width 2.20 nm with the edges functionalized by hydrogen atoms and hydroxy groups resulted from water decomposition.

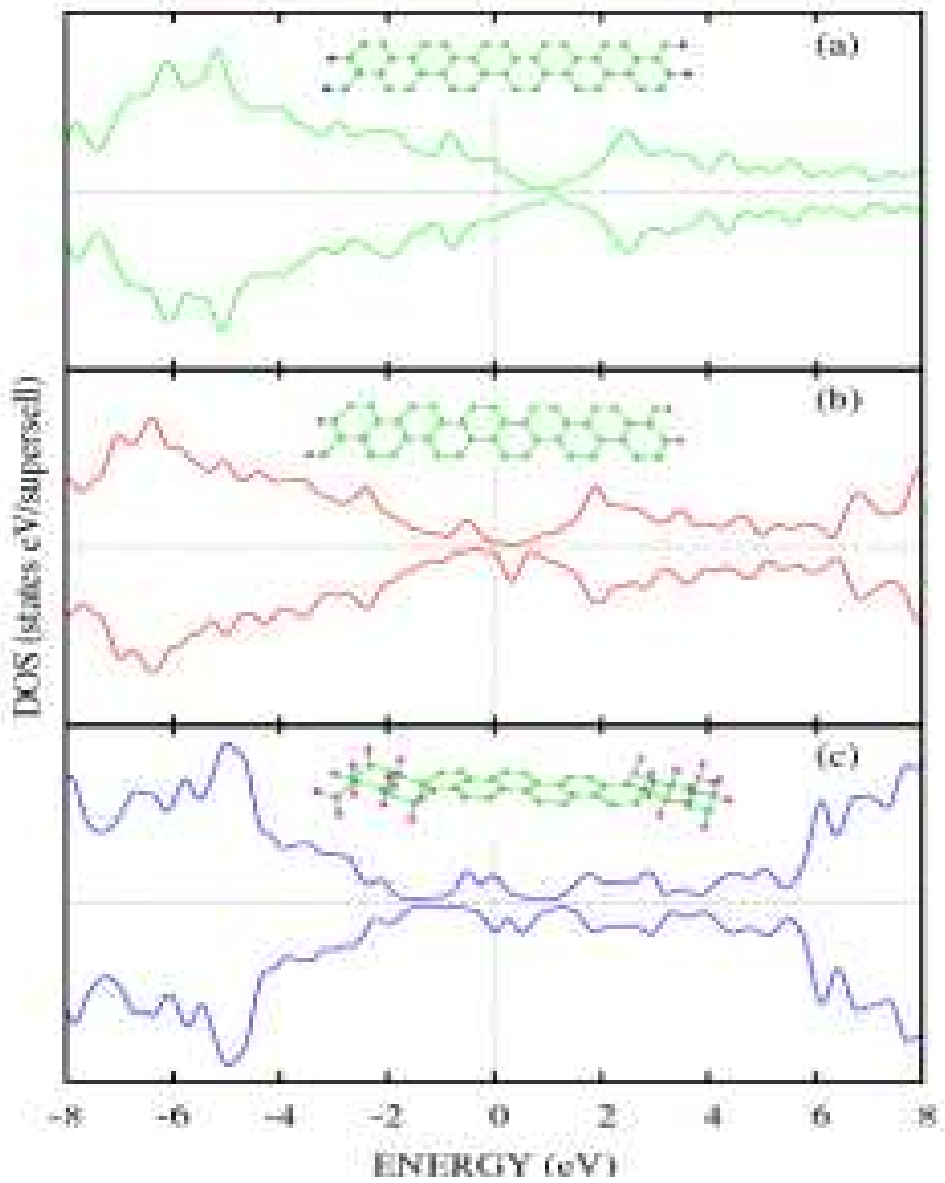

Figure 8: Densities of states for graphene nanoribbon of width of 2.2 nm with its edges functionalized by: (a) oxygen atoms and (b) hydrogen atoms; (c) the case of complete coverage of six first layers from the edges On insets optimized geometric structures of fuctionalized nanoribbons corresponding with dencities of states.

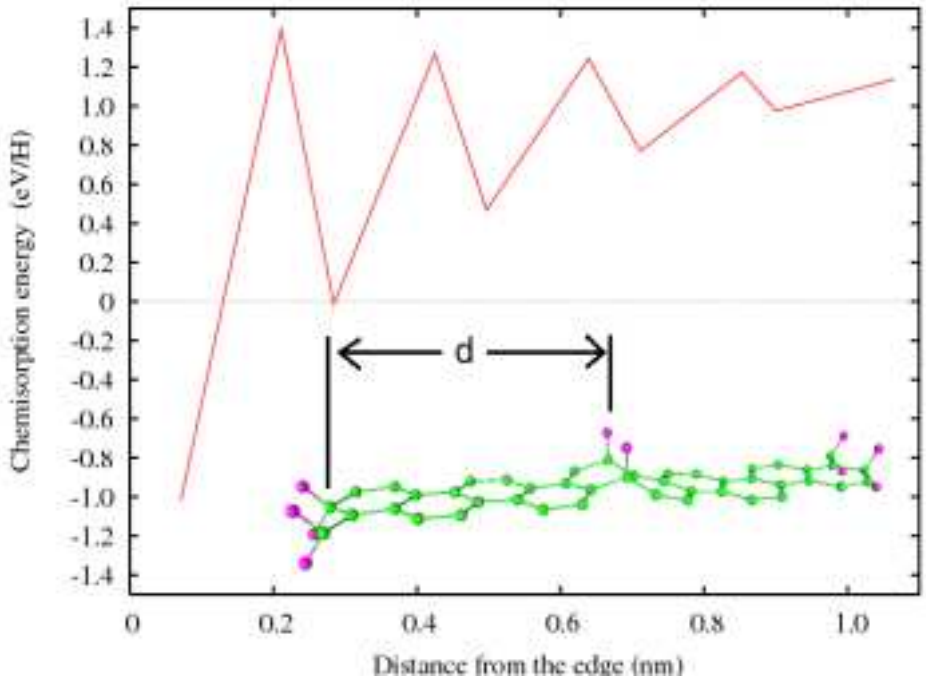

Figure 9: Chemisorption energy of hydrogen as a function of distance d from the edge. Inset: optimized geometric structure of the system under consideration.

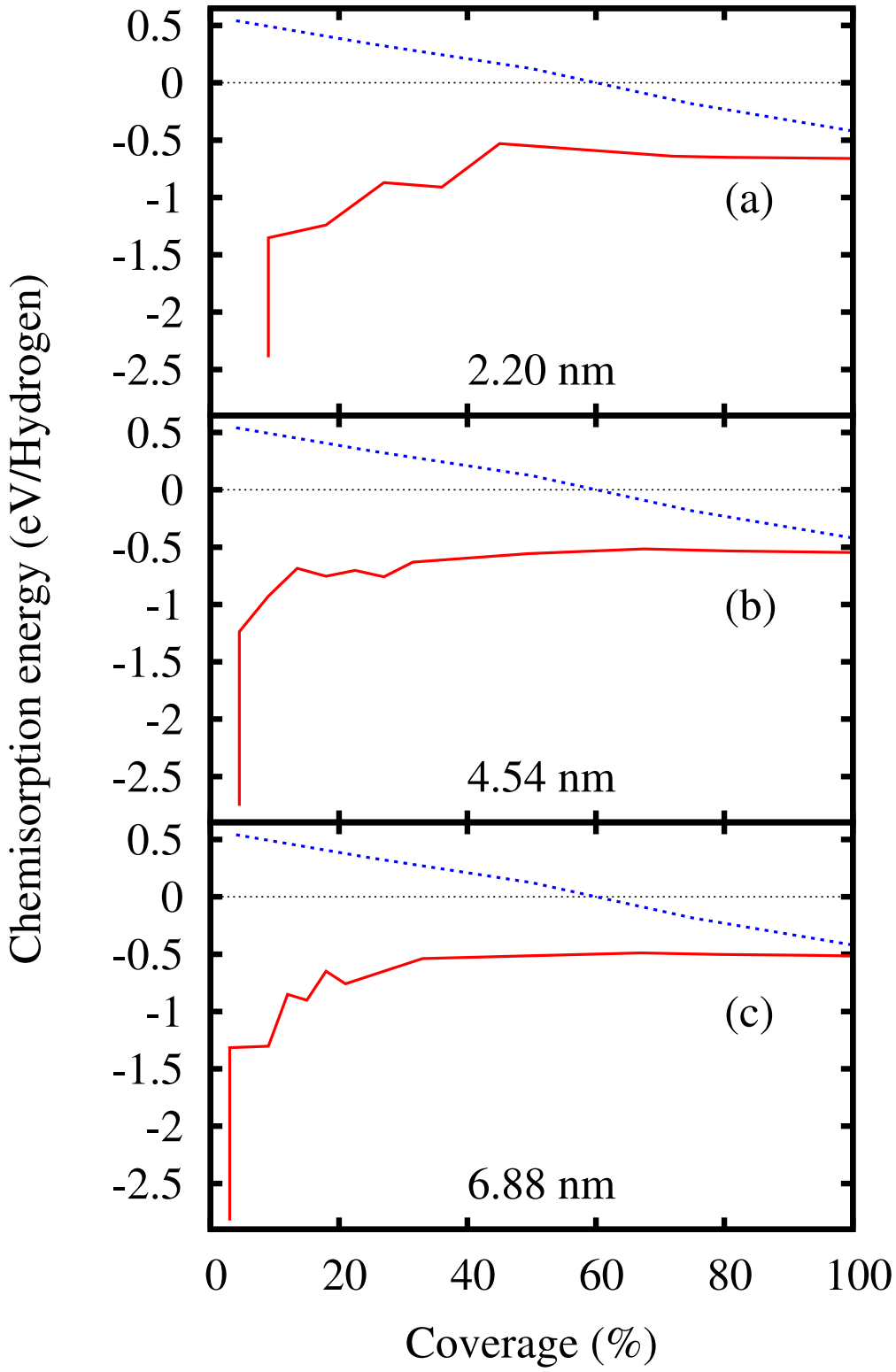

Figure 10: Formation energy as a function of coverage of graphene nanoribbons by hydrogen as a function of the nanoribbon width (red solid line). The blue dashed line presents the results for an ideal infinite graphene sheet.